Structural Engineering and Mechanics, *Vol. 69, No. 5 (2019) 479-486*
DOI: https://doi.org/10.12989/sem.2019.69.5.479

The finite element model of pre-twisted Euler beam based on general displacement solution

Ying Huang[1a], Changhong Chen*[2], Haoran Zou[2b] and Yao Yao[2c]

[1]*School of Civil Engineering, Xi'an University of Architecture and Technology, Xi'an, 710055, China*
[2]*School of Mechanics and Civil Engineering, Northwestern Polytechnical University, Xi'an, 710129, China*

(Received October 8, 2018, Revised January 10, 2019, Accepted January 13, 2019)

Abstract. Based on the displacement general solution of a pre-twisted Euler-Bernoulli beam, the shape function and stiffness matrix are deduced, and a new finite element model is proposed. Comparison analyses are made between the new proposed numerical model based on displacement general solution and the ANSYS solution by Beam188 element based on infinite approach. The results show that developed numerical model is available for the pre-twisted Euler-Bernoulli beam, and that also provide an accuracy finite element model for the numerical analysis. The effects of pre-twisted angle and flexural stiffness ratio on the mechanical property are also investigated.

Keywords: pre-twisted; Euler-Bernoulli beam; general solution; finite element; parametric analysis

1. Introduction

The pre-twisted beam, also known as a naturally twisted beam, presents an initially twisted shape in the natural state. Pre-twisted beams are widely used as structural elements. The blades of propellers, turbines and fans and drill bits are usually modelled as pre-twisted beams. Pre-twisted thin-walled members are being increasingly used in the construction of steel structure buildings and bridges. Based on the change rule of the pre-twisted angle along the beam axis, the pre-twisted beam can be divided into two cases: 1) Linear pre-twisted beam; 2) Non-linear pre-twisted beam (Zupan and Saje 2004). Based on the shape feature, the pre-twisted beam can be defined as the *n*th order pre-twisted beam when the pre-twisted angle ω is in the range of $(n-1)\pi,n\pi)$, (n=1, 2, …) (Fig. 1). Since a pre-twisted beam with small pre-twisted angle is dominant in application of civil engineering structures, the first order pre-twisted beam will be discussed in this paper, i.e., pre-twisted angle is in the range of $(0, 0.5\pi)$.

The early literature is mainly focused on stress analysis about the pre-twisted rod. Berdichevskii *et al.* (1985) investigated the stress state of a pre-twisted rod, and showed that the spatial problem can be successfully reduced to a Neumann-type problem for a certain system of second-order elliptic equations in the cross-section. The pre-twisted rods are decomposed into two independent problems, one bending and one extension-torsion. Recent research is focused on studying the vibration performance of pre-twisted blades and beams by using different techniques. A carefully selected sample of the relevant literature is as follows: Yoo *et al.* (2001) used a modeling method for the vibration analysis of rotating pre-twisted blades with a concentrated mass. Banerjee (2001, 2004) developed an exact dynamic stiffness method to predict the natural frequencies of a pre-twisted beam. Choi *et al.* (2007) studied bending vibration control of the pre-twisted rotating composite thin-walled beam based on a single cell composite beam. Sinha *et al.* (2011) derived the governing partial differential equation of motion for the transverse deflection of a rotating pre-twisted plate by using the thin shell theory. Adair and Jaeger (2017) analyzed a uniform pre-twisted rotating Euler-Bernoulli beam using the modified decomposition method. Fazayeli and Kharazi (2017) studied the effect of pre-twist on the nonlinear vibration of the blades considering the bending-bending-torsion coupling. Shenas *et al*. (2017) made research about carbon nanotube reinforced composite pre-twisted beams. Sachdeva *et al.* (2017) made models of initially curved and twisted smart beams using intrinsic equations. Karimi *et al.* (2018) analyzed Non-conservative stability of spinning pre-twisted cantilever beams. Chen *et al*. (2019) made vibration characteristics analysis to a rotating pre-twisted composite laminated blade. Li *et al.* (2019) made vibration control and analysis to a rotating flexible FGM beam with a lumped mass in temperature field.

The finite element technique has also been applied by many investigators, mostly for the vibration analysis of beams of uniform cross-section. All these investigations differ from one another in the nodal degrees of freedom

*Corresponding author, Associate Professor
E-mail: changhong.chen@nwpu.edu.cn
[a]Associate Professor
E-mail: cch-by@163.com
[b]M.Sc. Student
E-mail: zouhaoran@mail.nwpu.edu.cn
[c]Professor
E-mail: yaoy@nwpu.edu.cn

ISSN: 1225-4568 (Print), 1598-6217 (Online)

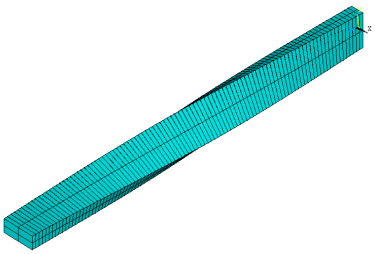

(a) $\omega = \pi / 2$

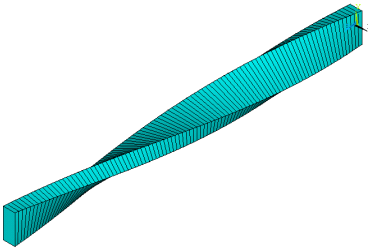

(b) $\omega = \pi$

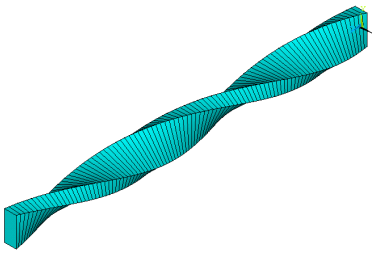

(c) $\omega = 2\pi$

Fig. 1 The beam model with different pre-twisted angle

taken for deriving the element stiffness and mass matrices. Chen and Keer (1993) studied the transverse vibration problems of a rotating twisted Timoshenko beam under axial loading and spinning about its axial axis, and investigated the effects of the twist angle, rotational speed, and axial force on natural frequencies by the finite element method. Nabi and Ganesan (1996) analyzed the vibration characteristics of pre-twisted metal matrix composite blades by using beam and plate theories. A beam element with eight degrees of freedom per node has been developed with torsion-flexure, flexure-flexure and shear-flexure couplings, which are encountered in twisted composite beams. A triangular plate element was used for the composite material to model the beam as a plate structure. Rao and Gupta (2001) derived the stiffness and mass matrices of a rotating twisted and tapered Timoshenko beam element, and calculated the first four natural frequencies and mode shapes in the bending-bending mode for cantilever beams.

However, as far as the authors are aware, only a few works have been reported in the existing literature on finite element formulation of pre-twisted beam based on coupled displacement fields (Tabarrok *et al.* 1988, Chen *et al.* 2014, 2016, 2018). The common finite element method to handle the static and dynamic problems of the pre-twisted beam is based on infinite approach strategy (ANSYS 2016). However, the polynomial displacement functions based on traditional straight beam do not correctly reflect the fact that the strain is zero when rigid motion occurs. Moreover, the

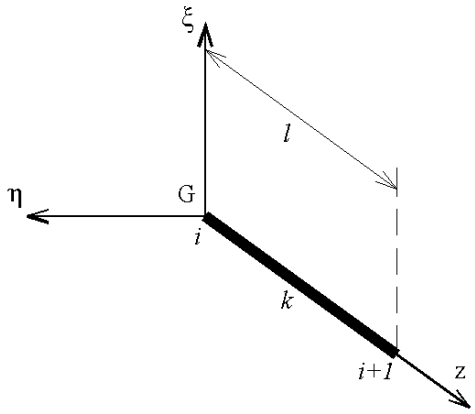

Fig. 2 The element of pre-twisted Euler-Bernoulli beam

fact that bending displacements are coupled with each other due to the naturally twisted angle ω will further cause new discretization error. Therefore, in the present study, a new finite element model based on displacement general solution of pre-twisted Euler-Bernoulli beam is derived.

2. The finite element model based on displacement general solution

2.1 The displacement function

The pre-twisted Euler-Bernoulli beam element model, whose length is l, and the pre-twisted angle rate is k, is studied in the local coordinate system G_$\xi\eta$z (Fig. 2). The displacements are u_i, v_i, w_i, $\varphi_{\xi i}$, $\varphi_{\eta i}$, φ_{zi} where the node is i, and the displacements are u_{i+1}, v_{i+1}, w_{i+1}, $\varphi_{\xi+1}$, $\varphi_{\eta+1}$, φ_{zi+1}, where node is i+1, respectively.

Supposing the pre-twisted element is constant strain element, the general displacement solution of pre-twisted Euler-Bernoulli beam is used as the displacement interpolation functions (Yu *et al.* 2002, Huang *et al.* 2017), as follows

$$[U]=[A]\begin{Bmatrix}[U_0]-[\Omega_R][\varphi_0]+\int_{z_i}^{z}[A]^T[\varepsilon]\mathrm{d}z-\\ [\Omega_R]\int_{z_i}^{z}[A]^T[K]\,\mathrm{d}z+\\ \int_{z_i}^{z}[\Omega_R][A]^T[K]\mathrm{d}z\end{Bmatrix} \tag{1}$$

$$[\varphi]=[A][\varphi_0]+[A]\int_{z_i}^{z}[A]^T[K]\mathrm{d}z$$

where $[A]=\begin{bmatrix}1 & 0 & 0\\ 0 & \cos kz & \sin kz\\ 0 & -\sin kz & \cos kz\end{bmatrix}$, which is the coordinate transformation matrix. $[U_0]$, $[\varphi_0]$, $[K]$ and $[\varepsilon]$ are undetermined constant strain vectors, respectively; $[\Omega_R]$ is the dual-antisymmetric matrix generated by the vector $[R]=[Z]-[Z_i]$; $[Z_i]$ represents position vector $[Z]$ when $z=z_i$, namely $[Z_i]=[Z]_{z=z_i}$.

When z is equal to z_i, the Eq. (1) can be simplified to the following

$$[U_0]=[A_i]^T[U_i],\ [\varphi_0]=[A_i]^T[\varphi_i] \tag{2}$$

where $[U_i]=[U]_{z=z_i}$, $[\varphi_i]=[\varphi]_{z=z_i}$, $[A_i]=[A]_{z=z_i}$.

When z is equal to z_{i+1}, the Eq. (1) can be simplified to the following

$$\begin{aligned}&[A_{i+1}]^T[U_{i+1}]-[A_i]^T[U_i]+[\Omega_{R_{i+1}}]\\&[A_i]^T[\varphi_i]=\int_{z_i}^{z_{i+1}}[A]^T[\varepsilon]\mathrm{d}z+\\&\int_{z_i}^{z_{i+1}}[\Omega_R][A]^T[K]\mathrm{d}z-[\Omega_{R_{i+1}}]\\&\int_{z_i}^{z_{i+1}}[A]^T[K]\mathrm{d}z\end{aligned} \tag{3}$$

$$[A_{i+1}]^T[\varphi_{i+1}]-[A_i]^T[\varphi_i]=\int_{z_i}^{z_{i+1}}[A]^T[K]\mathrm{d}z \tag{4}$$

where $[\Omega_{R_{i+1}}]$ is the dual-antisymmetric matrix generated by the vector $[R_{i+1}]=[Z_{i+1}]-[Z_i]$.

The constant strain matrix $[K]$ is obtained by the Eq. (4), as follows

$$\begin{aligned}&[K]=(\int_{z_i}^{z_{i+1}}[A]^T\mathrm{d}z)^{-1}([A_{i+1}]^T[\varphi_{i+1}]\\&-[A_i]^T[\varphi_i])\end{aligned} \tag{5}$$

Substituting (5) into (3), the following Eq. (6) can be obtained

$$\begin{aligned}&[A_{i+1}]^T[U_{i+1}]-[A_i]^T[U_i]+[\Omega_{R_{i+1}}]\\&[A_{i+1}]^T[\varphi_{i+1}]=\int_{z_i}^{z_{i+1}}[A]^T[\varepsilon]\mathrm{d}z+\\&\int_{z_i}^{z_{i+1}}[\Omega_R][A]^T[K]\mathrm{d}z\end{aligned} \tag{6}$$

The constant strain matrix $[\varepsilon]$ is obtained by substituting (5) into (6), as

$$[\varepsilon]=\begin{bmatrix}[T_{11}] & [T_{12}] & [T_{13}] & [T_{14}]\end{bmatrix}\cdot\begin{bmatrix}[U_i]\\[\varphi_i]\\[U_{i+1}]\\[\varphi_{i+1}]\end{bmatrix} \tag{7}$$

where

$$\begin{aligned}[T_{11}]&=-\left(\int_{z_i}^{z_{i+1}}[A]^T\mathrm{d}z\right)^{-1}[A_i]^T\\[T_{12}]&=\left(\int_{z_i}^{z_{i+1}}[A]^T\mathrm{d}z\right)^{-1}\int_{z_i}^{z_{i+1}}[\Omega_R][A]^T\\&\left(\int_{z_i}^{z_{i+1}}[A]^T\mathrm{d}z\right)^{-1}[A_i]^T\mathrm{d}z\\[T_{13}]&=\left(\int_{z_i}^{z_{i+1}}[A]^T\mathrm{d}z\right)^{-1}[A_{i+1}]^T\end{aligned}$$

$$[T_{14}]=\left(\int_{z_i}^{z_{i+1}}[A]^T\mathrm{d}z\right)^{-1}\left\{\begin{aligned}&[\Omega_{R_{i+1}}][A_{i+1}]^T-\\&\int_{z_i}^{z_{i+1}}[\Omega_R][A]^T\\&\left(\int_{z_i}^{z_{i+1}}[A]^T\mathrm{d}z\right)^{-1}[A_{i+1}]^T\mathrm{d}z\end{aligned}\right\}$$

Similarly, the Eq. (5) can be expressed by node displacements as

$$[K]=\begin{bmatrix}[T_{21}] & [T_{22}] & [T_{23}] & [T_{24}]\end{bmatrix}\cdot\begin{bmatrix}[U_i]\\[\varphi_i]\\[U_{i+1}]\\[\varphi_{i+1}]\end{bmatrix} \tag{8}$$

where

$$\begin{aligned}[T_{21}]&=[0]\\[T_{22}]&=-\left(\int_{z_i}^{z_{i+1}}[A]^T\mathrm{d}z\right)^{-1}[A_i]^T\\[T_{23}]&=[0]\\[T_{24}]&=\left(\int_{z_i}^{z_{i+1}}[A]^T\mathrm{d}z\right)^{-1}[A_{i+1}]^T\end{aligned}$$

The total constant strain matrix is by the Eqs. (7) and (8)

$$\begin{bmatrix}\varepsilon\\K\end{bmatrix}=[T]\cdot\begin{bmatrix}[U_i]\\[\varphi_i]\\[U_{i+1}]\\[\varphi_{i+1}]\end{bmatrix} \tag{9}$$

where $[T]=\begin{bmatrix}[T_{11}] & [T_{12}] & [T_{13}] & [T_{14}]\\[T_{21}] & [T_{22}] & [T_{23}] & [T_{24}]\end{bmatrix}$.

The displacement function can be obtained by substituting the Eq. (9) into Eq. (1), as follows

$$\begin{bmatrix}[U]\\[\varphi]\end{bmatrix}=[N]\cdot\begin{bmatrix}[U_i]\\[\varphi_i]\\[U_{i+1}]\\[\varphi_{i+1}]\end{bmatrix} \tag{10}$$

where the shape function is

$$[N]=\begin{bmatrix}[N_{11}] & [N_{12}] & [N_{13}] & [N_{14}]\\[N_{21}] & [N_{22}] & [N_{23}] & [N_{24}]\end{bmatrix} \tag{11}$$

where

$$[N_{11}]=[A]\left([A_i]^T+[T_{11}]\int_{z_i}^{z}[A]^T\mathrm{d}z\right)$$

$$[N_{12}]=[A]\left\{\begin{aligned}&-[\Omega_R][A_i]^T+[T_{12}]\\&\int_{z_i}^{z}[A]^T\mathrm{d}z+[T_{22}]\left(\int_{z_i}^{z}[\Omega_R][A]^T\mathrm{d}z\right.\\&\left.-[\Omega_R]\int_{z_i}^{z}[A]^T\mathrm{d}z\right)\end{aligned}\right\}$$

$$[N_{13}]=[A][T_{13}]\int_{z_i}^{z}[A]^T\mathrm{d}z$$

$$[N_{14}]=[A]\left\{\begin{array}{c}[A]^T\,\mathrm{d}z+\\ [T_{14}]\int_{z_i}^{z}[T_{24}]\left(\int_{z_i}^{z}[\Omega_R][A]^T\,\mathrm{d}z-\right.\\ \left.\int_{z_i}^{z}[\Omega_R]\int_{z_i}^{z}[A]^T\,\mathrm{d}z\right)\end{array}\right\}$$

$$[N_{21}]=[0]$$

$$[N_{22}]=[A][T_{22}]\int_{z_i}^{z}[A]^T\,\mathrm{d}z$$

$$[N_{23}]=[0]$$

$$[N_{24}]=[A][T_{24}]\int_{z_i}^{z}[A]^T\,\mathrm{d}z$$

2.2 The element stiffness matrix

The strain energy per unit length of pre-twisted Euler-Bernoulli beam under small deformation conditions is as follows

$$\Gamma=\iint_A\frac{1}{2}(\sigma_z\varepsilon_z+\tau_{z\xi}\gamma_{z\xi}+\tau_{z\eta}\gamma_{z\eta})\mathrm{d}\xi\mathrm{d}\eta \tag{12}$$

Based on the strain relations of pre-twisted Euler-Bernoulli beam (Banerjee 2004, Chen *et al.* 2014, 2016), as follows

$$\begin{cases}\gamma_{z\xi}=-\varphi_\eta+u'-kv-\eta\varphi_z'\\ \gamma_{z\eta}=\varphi_\xi+v'+ku+\xi\varphi_z'\\ \varepsilon_z=w'-\xi(\varphi_\eta'+k\varphi_\xi)+\eta(\varphi_\xi'-k\varphi_\eta)\end{cases} \tag{13}$$

and considering the following relations between internal force and stress (Yu *et al*. 2002)

$$\begin{bmatrix}N\\Q_\xi\\Q_\eta\end{bmatrix}=\iint_A\begin{bmatrix}\sigma_z\\\tau_{z\xi}\\\tau_{z\eta}\end{bmatrix}\mathrm{d}\xi\mathrm{d}\eta\,,\ \begin{bmatrix}M_z\\M_\xi\\M_\eta\end{bmatrix}=\iint_A\begin{bmatrix}\xi\tau_{z\eta}-\eta\tau_{z\xi}\\\eta\sigma_z\\-\xi\sigma_z\end{bmatrix}\mathrm{d}\xi\mathrm{d}\eta \tag{14}$$

substituting Eqs. (13) and (14) into (12), the strain energy can be obtained

$$\Gamma=\frac{1}{2}[\varepsilon]^T[N]+\frac{1}{2}[K]^T[M] \tag{15}$$

where

$$[\varepsilon]=\begin{bmatrix}\varepsilon\\\gamma_\xi\\\gamma_\eta\end{bmatrix},\ [K]=\begin{bmatrix}k_z\\k_\xi\\k_\eta\end{bmatrix},\ [N]=\begin{bmatrix}N\\Q_\xi\\Q_\eta\end{bmatrix},\ [M]=\begin{bmatrix}M_z\\M_\xi\\M_\eta\end{bmatrix},$$

$$\begin{cases}\varepsilon=w'\\ \gamma_\xi=-\varphi_\eta+u'-kv\\ \gamma_\eta=\varphi_\xi+v'+ku\end{cases},\quad\begin{cases}k_\xi=\varphi_\xi'-k\varphi_\eta\\ k_\eta=\varphi_\eta'+k\varphi_\xi\\ k_z=\varphi_z'\end{cases}$$

Based on equivalent constitutive equation of pre-twisted beam, the strain energy can be expressed as

$$\Gamma=\frac{1}{2}[\varepsilon]^T[B][\varepsilon]+\frac{1}{2}[K]^T[D][K] \tag{15}$$

where

$$[B]=\begin{bmatrix}EA&0&0\\0&GA&0\\0&0&GA\end{bmatrix},\ [\mathrm{D}]=\begin{bmatrix}GJ&0&0\\0&EI_\xi&0\\0&0&EI_\eta\end{bmatrix}$$

The total potential energy of the pre-twisted beam element based on energy principle is as follows

$$\begin{aligned}\Pi=&\int_{z_i}^{z_{i+1}}\Gamma\mathrm{d}z-\int_{z_i}^{z_{i+1}}[\mathrm{U}]^{\mathrm{T}}[\mathrm{p}]\mathrm{d}z\\ &-\int_{z_i}^{z_{i+1}}[\varphi]^{\mathrm{T}}[\mathrm{m}]\mathrm{d}z-[\mathrm{U}]^{\mathrm{T}}[\bar{\mathrm{p}}]\Big|_{z_i}^{z_{i+1}}-[\varphi]^{\mathrm{T}}[\bar{\mathrm{m}}]\Big|_{z_i}^{z_{i+1}}\end{aligned} \tag{16}$$

where $[p]$, $[\mathrm{m}]$, $[\bar{\mathrm{p}}]$, $[\bar{\mathrm{m}}]$ represent linear distribution load vector, distribution moment load vector, node concentrated load vector and node concentrated moment vector, respectively. The Eq. (17) can be expressed as the following by substituting Eqs. (9), (10) and (16) into (17)

$$\begin{aligned}\Pi=&\int_{z_i}^{z_{i+1}}\frac{1}{2}[\varepsilon]^{\mathrm{T}}[\mathrm{B}][\varepsilon]\mathrm{d}z+\int_{z_i}^{z_{i+1}}\frac{1}{2}[K]^{\mathrm{T}}[D][K]\mathrm{d}z\\ &-\int_{z_i}^{z_{i+1}}[U]^{\mathrm{T}}[p]\mathrm{d}z-\int_{z_i}^{z_{i+1}}[\varphi]^{\mathrm{T}}[m]\mathrm{d}z-[U]^{\mathrm{T}}[\bar{p}]\Big|_{z_i}^{z_{i+1}}-[\varphi]^{\mathrm{T}}[\bar{m}]\Big|_{z_i}^{z_{i+1}}\\ =&\frac{1}{2}\begin{bmatrix}[U_i]\\[\varphi_i]\\[U_{i+1}]\\[\varphi_{i+1}]\end{bmatrix}^T\left(\int_{z_i}^{z_{i+1}}[T]^T\begin{bmatrix}[B]&\\&[D]\end{bmatrix}[T]\mathrm{d}z\begin{bmatrix}[U_i]\\[\varphi_i]\\[U_{i+1}]\\[\varphi_{i+1}]\end{bmatrix}-\int_{z_i}^{z_{i+1}}[N]^T\begin{bmatrix}[\mathrm{p}]\\[\mathrm{m}]\end{bmatrix}\mathrm{d}z-\left[\begin{bmatrix}[\bar{\mathrm{p}}]\\[\bar{\mathrm{m}}]\end{bmatrix}\right]_{z_i}^{z_{i+1}}\right)\end{aligned} \tag{17}$$

Based on the principle of minimum potential energy, the stiffness and equivalent node load matrix are obtained as

$$[R]^e=\int_{z_i}^{z_{i+1}}[N]^T\begin{bmatrix}[p]\\[m]\end{bmatrix}dz-\left[\begin{bmatrix}[\bar{p}]\\[\bar{m}]\end{bmatrix}\right]_{z_i}^{z_{i+1}} \tag{18}$$

$$[k]^e=l_i[T]^T\begin{bmatrix}[B]&\\&[D]\end{bmatrix}[T] \tag{19}$$

3. The analysis example and discussion

The analysis model for our example is a cantilever beam, whose length l is 6000 mm; the cross-section is a rectangular (Fig. 3): the height h is 500 mm, the width is 200 mm. The pre-twisted angle ω is 0.5π. The steel elastic modulus E is $2.0\times10^5\,Mpa$ and Poisson's ratio is 0.3. The concentrated force P is 50 kN, and the self-weight of beam is not considered in this case. The load vectors in this example are $[\mathrm{p}]=[\mathrm{m}]=[\bar{\mathrm{m}}]=(0,0,0)^T$ and $[\bar{\mathrm{p}}]=(0,-50e3,0)^T$.

3.1 The effect of element size of using ANSYS model

Based on the infinite approach method and ANSYS software (ANSYS 2016), the finite element model is established. The element type is Beam188 (Fig. 4), the warping degree of freedom is ignored (K1=0, Unrestrained), and a cubic form shape function is used (K3=3). As the beam188 is a Timoshenko beam element, and to compare with above Euler-Bernoulli beam model, this paper amplifies the original shear stiffness (GA=7.692e9) through multiplication by the coefficient 10^5 (Fig. 5).

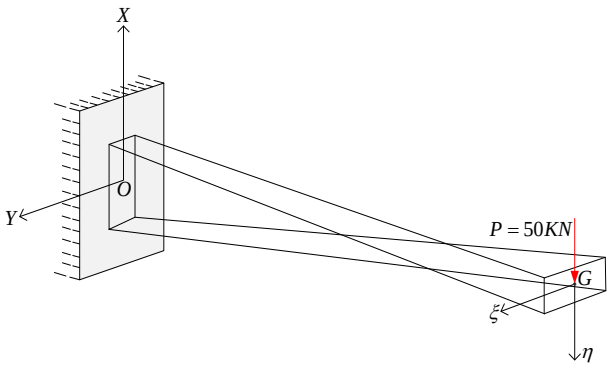

Fig. 3 The geometric parameter with rectangular cross section

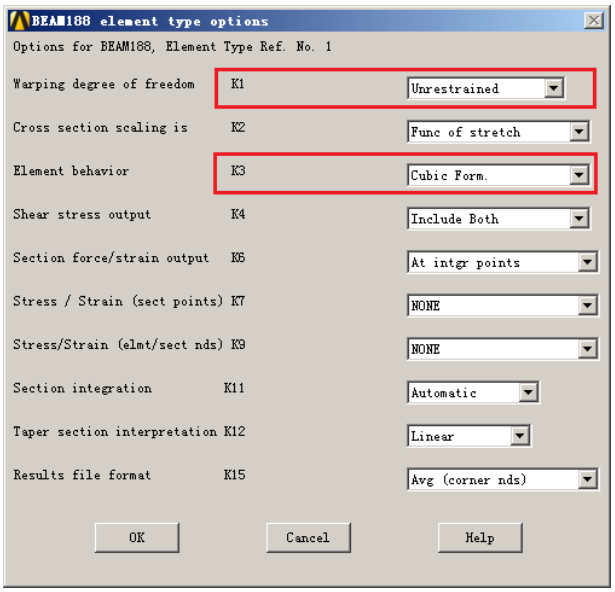

Fig. 4 The beam188 element type options

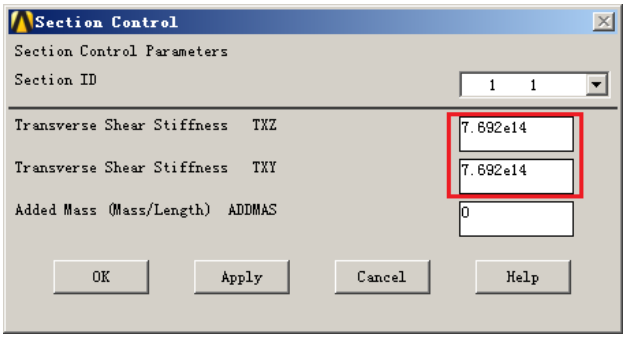

Fig. 5 The amplification of shear stiffness

The cubic form shape function chosen means that the analysis result is precise when considering the classic straight beam (ω=0). However, this method using the infinite approach has obvious rotation discretization errors when pre-twisted angle is not equal to zero (Fig. 6), and more elements must be used to decrease this discretization error. Based on displacement results of the end of the beam (Fig. 7), the deviation of displacement is very small and almost zero when number of elements n is greater than 20 for this analysis case.

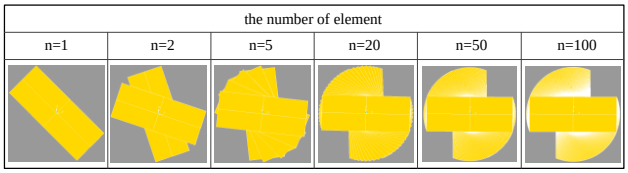

Fig. 6 The rotation discretization error (ω=0.5π)

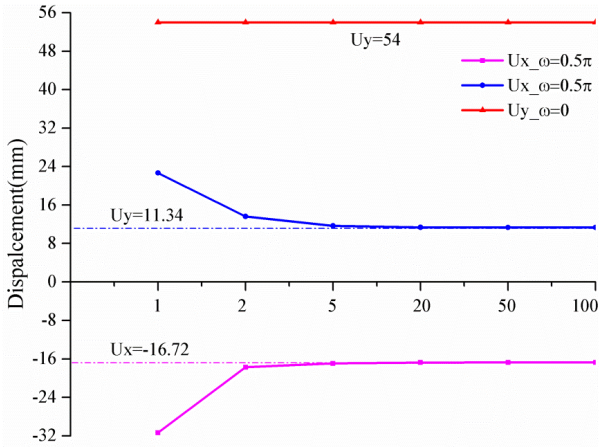

(a) The linear displacement comparison at the end of beam

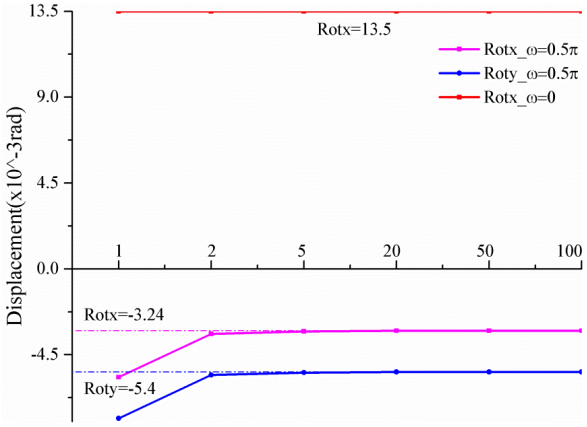

(b) The rotation displacement comparison at the end of beam

Fig. 7 The displacement comparison at the end of beam

3.2 The effect of element size of the proposed model

For further testing the effect of element size on results, the different element sizes of the proposed numerical model based on displacement general solution will be used to validate this model; namely, the cantilever beam is divided into 1,2,5,20,50,100 equal parts, respectively. The displacement comparison results at the end of beam are as shown in Fig. 8, which also indicates that the displacement deviation is very small and almost zero when the number of element n is greater than 20.

3.3 The comparison of displacement results

The displacement comparisons between the proposed model based on displacement general solution and the ANSYS model are as follows (Fig. 9), the number of elements used is 50.

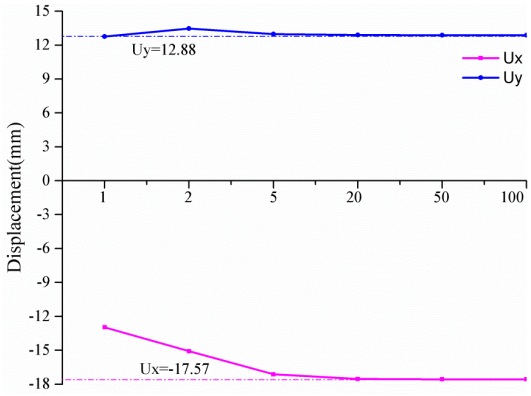

(a) The linear displacement comparison at the end of beam

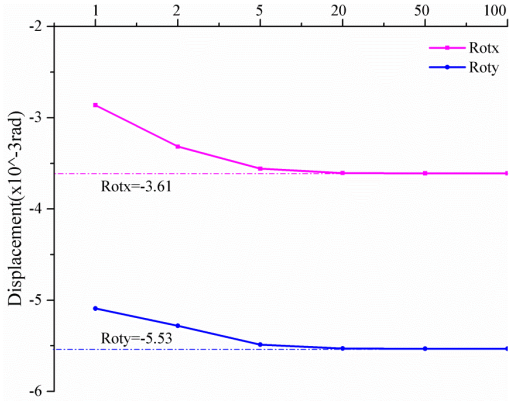

(b) The rotation displacement comparison at the end of beam

Fig. 8 The displacement comparison at the end of beam

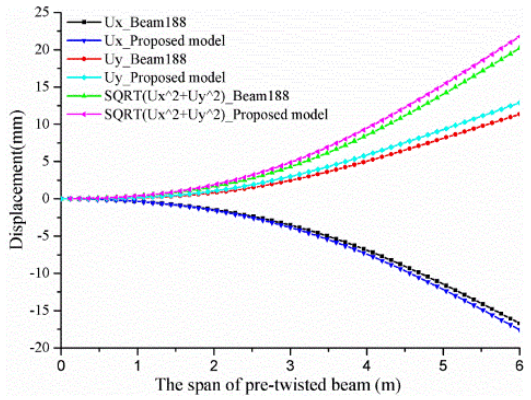

(a) The linear displacements comparison

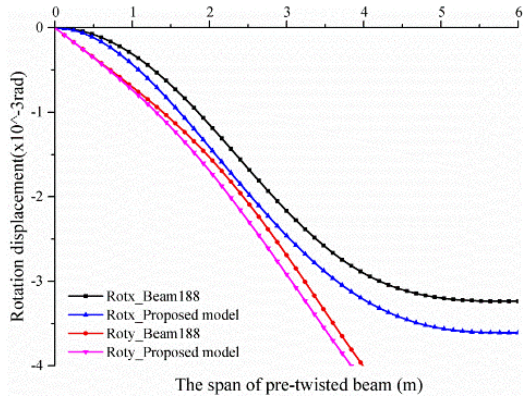

(b) The rotation displacements comparison

Fig. 9 The displacements comparison

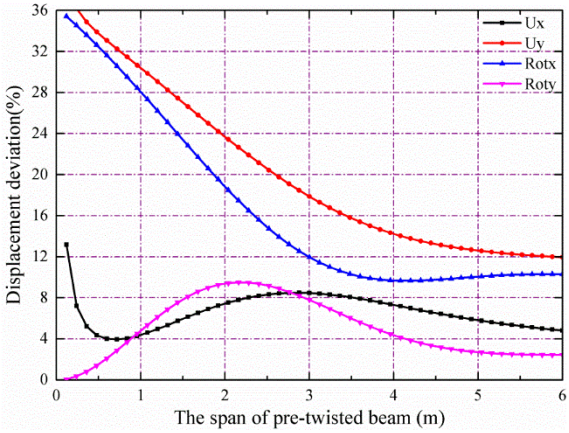

Fig. 10 The displacement deviation

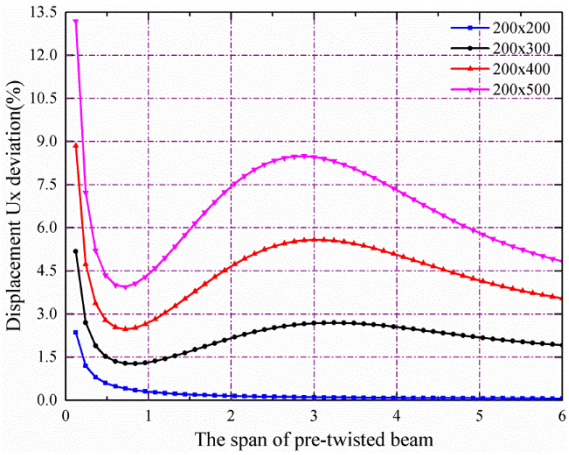

(a) The displacement Ux deviation comparison

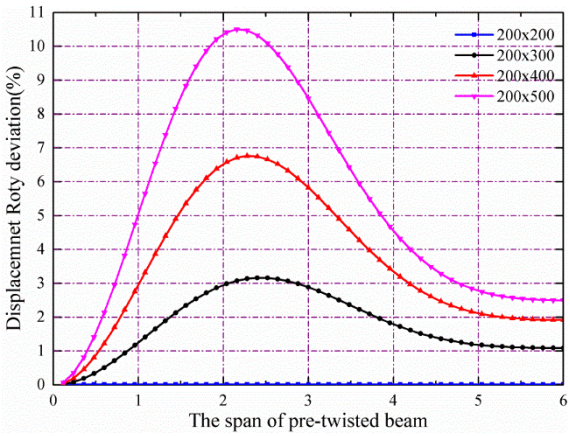

(b) The displacement Roty deviation comparison

Fig. 11 The displacement deviation comparison

The trends of displacement change are almost same between the ANSYS model and the proposed numerical model of this paper. The lateral displacements couple with each other because of the existence of pre-twisted angle ω, namely, the lateral linear displacement Uy and rotation displacement Roty will arise (Fig. 9). The results of displacement deviation also indicate that the deviations of main displacement Ux and Roty corresponding to force P are smaller than secondary displacement Uy and Rotx (Fig. 10).

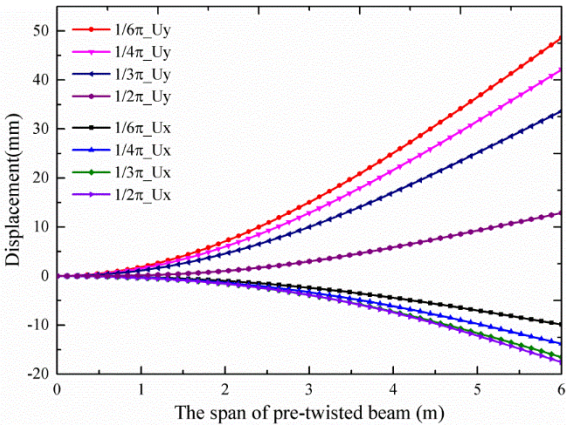

(a) The linear displacement comparison

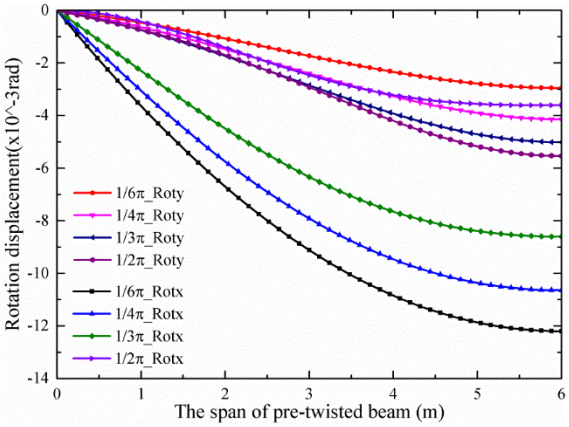

(b) The rotation displacement comparison

Fig. 12 The displacement comparison

To further investigate the deviation error of these two models, the comparison analyses by using different section sizes (200×200, 200×300, 200×400, and 200×500, respectively) are conducted. The results indicate that displacement deviations will be smaller and smaller as the flexural stiffness along two main axis directions become closer and closer (Fig. 11). This again indicates that the nature of the method based on infinite approach is just a decomposition of moment of inertia between the two main axial directions, and the nonlinear coupled effect is not considered.

4. Parametric analysis

4.1 The effect of pre-twisted angle on deflections

The effect of pre-twisted angle ω on the deflections has been investigated (Fig. 12) and it is shown that the displacement Ux corresponding to the main axis $G\eta$ increased gradually with increasing of the pre-twisted angle, and the displacement Uy corresponding to the secondary axis $G\xi$ is also increased. The equivalent stiffness is also shown to be decreased along main axis direction as the increment of pre-twisted angle, and then the displacement is increased when the pre-twisted angle changes in the range of $[0,0.5\pi]$. The displacements along main axis and

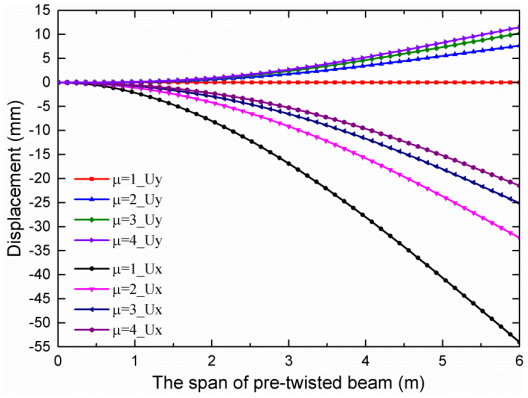

(a) The linear displacement comparison

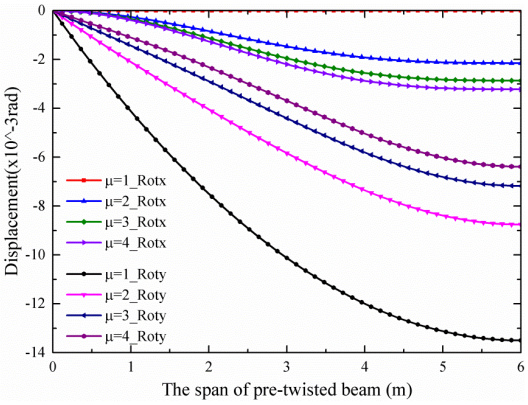

(b) The rotation displacement comparison

Fig. 13 The displacement comparison

secondary axis direction are coupled to each other because of the existence of pre-twisted angle. The coupling effect will become stronger, and the lateral displacement Uy will also be increased with the increasing of pre-twisted angle.

4.2 The effect of flexural stiffness ratio on deflections

The flexural stiffness ratio of pre-twisted beam with isotropic material is introduced as follows

$$\mu = \frac{I_\eta}{I_\xi} \geq 1 \tag{21}$$

Using the above example in the 3 section and assuming that the flexural stiffness EI_ξ along secondary axis $G\xi$ direction remains unchanged, the effect of the parameter μ on deflections has been investigated by changing the flexural stiffness ratio μ from 1 to 4 (Fig. 13). The results show that the displacements Ux and Roty decreased corresponding to main axis $G\eta$, while the displacements Uy and Rotx increased corresponding to secondary axis $G\xi$ with the increasing of flexural stiffness ratio μ. The coupling effect of the pre-twisted beam becomes stronger between the strong axis and secondary axis as the flexural stiffness ratio μ increased.

5. Conclusions

- Based on the displacement general solution of a pre-

twisted Euler-Bernoulli beam, the shape functions and stiffness matrix are deduced, and a precise finite element model is proposed.

• By comparison with ANSYS solution by using straight Beam188 element based on infinite approach method, the results show that the proposed model is available for pre-twisted beam and provides an accuracy displacement interpolation function for the finite element analysis.

• The effects of pre-twisted angle and flexural stiffness ratio on deflections have been investigated. The displacements along main axis and secondary axis directions are coupled to each other because of the existence of the pre-twisted angle. The equivalent flexural stiffness decreased along main axis direction as the increment of pre-twisted angle when the pre-twisted angle changes in the range of $[0,0.5\pi]$.

Acknowledgements

The authors would like to acknowledge the financial support by the National Natural Science Foundation of China (51408489, 51248007, 51308448 and 11572249), the China Scholarship Council (201606295016), the Shaanxi National Science Foundation of China (2017JM5007), and the Top International University Visiting Program for Outstanding Young Scholars of Northwestern Polytechnical University.

References

Adair, D. and Jaeger, M. (2017), "Vibration analysis of a uniform pre-twisted rotating Euler-Bernoulli beam using the modified Adomian decomposition method", *Math. Mech. Sol.*, **23**(9), 1345-1363.

ANSYS Inc. (2016), *ANSYS Programmer's Guide Release 14.0*, 1st Edition, U.S.A.

Banerjee, J.R. (2001), "Free vibration analysis of a twisted beam using the dynamic stiffness method", *Int. J. Sol. Struct.*, **38**(38), 6703-6722.

Banerjee, J.R. (2004), "Development of an exact dynamic stiffness matrix for free vibration analysis of a twisted Timoshenko beam", *J. Sound Vibr.*, **270**(1), 379-401.

Berdichevskii, V.L. and Starosel'skii, L.A. (1985), "Bending, extension, and torsion of naturally twisted rods", *J. Appl. Math. Mech.*, **49**(6), 746-755.

Chen, C.H., Yao, Y. and Huang, Y. (2014), "Elastic flexural and torsional buckling behavior of pre-twisted bar under axial load", *Struct. Eng. Mech.*, **49**(2), 273-283.

Chen, C.H., Zhu, Y.F., Yao, Y. and Huang, Y. (2016), "Progressive collapse analysis of steel frame structure based on the energy principle", *Steel Compos. Struct.*, **21**(3), 553-571.

Chen, C.H., Zhu, Y.F., Yao, Y. and Huang, Y. (2016), "The finite element model research of the pre-twisted thin-walled beam", *Struct. Eng. Mech.*, **57**(3), 389-402.

Chen, C.H., Zhu, Y.F., Yao, Y., Huang, Y. and Long, X. (2016), "An evaluation method to predict progressive collapse resistance of steel frame structures", *J. Constr. Steel Res.*, **122**, 238-250.

Chen, C., Gong, H., Yao, Y., Huang, Y. and Keer, L.M. (2018), "Investigation on the seismic performance of T-shaped column joints", *Comput. Concrete*, **21**(3), 335-344.

Chen, C., Zhang, Q., Keer, L.M., Yao, Y. and Huang, Y. (2018), "The multi-factor effect of tensile strength of concrete in numerical simulation based on the Monte Carlo random aggregate distribution", *Constr. Build. Mater.*, **165**, 585-595.

Chen, J. and Li, Q.S. (2019), "Vibration characteristics of a rotating pre-twisted composite laminated blade", *Compos. Struct.*, 208, 78-90.

Chen, W.R. and Keer, L.M. (1993), "Transverse vibrations of a rotating twisted Timoshenko beam under axial loading", *J. Vibr. Acoust.*, **115**(3), 285-294.

Choi, S.C., Park, J.S. and Kim, J.H. (2007), "Vibration control of pre-twisted rotating composite thin-walled beams with piezoelectric fiber composites", *J. Sound Vibr.*, **300**(1), 176-196.

Fazayeli, H. and Kharazi, M. (2017), "Effect of pre-twist on the nonlinear vibration of the blades considering the bending-bending-torsion coupling", *Proceedings of the 8th International Conference on Mechanical and Aerospace Engineering*, Prague, Czech Republic, July.

Huang, Y., Chen, C.H., Leon, M.K. and Yao, Y. (2017), "A general solution to structural performance of pre-twisted Euler beam subject to static load", *Struct. Eng. Mech.*, **64**(2), 205-212.

Karimi-Nobandegani, A., Fazelzadeh, S.A. and Ghavanloo, E. (2018), "Non-conservative stability of spinning pretwisted cantilever beams", *J. Sound Vibr.*, **412**, 130-147.

Li, L., Liao, W.H., Zhang, D. and Zhang, Y. (2019), "Vibration control and analysis of a rotating flexible FGM beam with a lumped mass in temperature field", *Compos. Struct.*, **208**, 244-260.

Mustapha, K.B. (2017), "Dynamic behaviors of spinning pre-twisted Rayleigh micro-beams", *Eur. J. Comput. Mech.*, **26**(5-6), 473-507.

Nabi, S.M. and Ganesan, N. (1996), "Comparison of beam and plate theories for free vibrations of metal matrix composite pre-twisted blades", *J. Sound Vibr.*, **189**(2), 149-160.

Rao, S.S. and Gupta, R.S. (2001), "Finite element vibration analysis of rotating Timoshenko beams", *J. Sound Vibr.*, **242**(1), 103-124.

Sachdeva, C., Gupta, M. and Hodges, D.H. (2017), "Modeling of initially curved and twisted smart beams using intrinsic equations", *Int. J. Sol. Struct.*, **148**, 3-13.

Shenas, A.G., Malekzadeh, P. and Ziaee, S. (2017), "Vibration analysis of pre-twisted functionally graded carbon nanotube reinforced composite beams in thermal environment", *Compos. Struct.*, **162**, 325-340.

Shenas, A.G., Ziaee, S. and Malekzadeh, P. (2017), "Nonlinear vibration analysis of pre-twisted functionally graded microbeams in thermal environment", *Thin-Wall. Struct.*, **118**, 87-104.

Sinha, S.K. and Turner, K.E. (2011), "Natural frequencies of a pre-twisted blade in a centrifugal force field", *J. Sound Vibr.*, **330**(11), 2655-2681.

Tabarrok, B., Farshad, M. and Yi, H. (1988), "Finite element formulation of spatially curved and twisted rods", *Comput. Meth. Appl. Mech. Eng.*, **70**(3), 275-299.

Yoo, H.H., Kwak, J.Y. and Chung, J. (2001), "Vibration analysis of rotating pre-twisted blades with a concentrated mass", *J. Sound Vibr.*, **240**(5), 891-908.

Yu, A., Fang, M. and Ma, X. (2002), "Theoretical research on naturally curved and twisted beams under complicated loads", *Comput. Struct.*, **80**(32), 2529-2536.

Zupan, D. and Saje, M. (2004), "On a proposed standard set of problems to test finite element accuracy: The twisted beam", *Fin. Elem. Analy. Des.*, **40**(11), 1445-1451

CC